of both iron and copper targets are required to resolve these differences.

Natural Production of Tritium

Two problems involving the formation of tritium in high-energy nuclear reactions are of particular interest: the formation by cosmic rays in meteorites and in the atmosphere. Since the tritium-production cross sections are constant above 0.450 Bev for nitrogen and oxygen and constant above 2 Bev for iron, the discussion which appeared in reference 1 is essentially unaltered. Recent measurements of tritium in nature, however, have considerably altered the agreement between the observed tritium production in the atmosphere and that predicted on the basis of the cosmic-ray reactions.[11] The predicted tritium flux remains at about 0.14 t/cm^2-sec, whereas the observed flux may be $2.0\pm(50\%)$ t/cm^2-sec.[12] Possible sources for the discrepancy include: a higher flux of incident cosmic rays, additional tritium-producing reactions, influx of tritons with the cosmic rays, more serious secondary production of tritium in the atmosphere, and unsuspected loss of tritium from the targets.

ACKNOWLEDGMENTS

The author wishes to thank Dr. P. Benioff, Dr. M. Kalkstein, Dr. G. T. Seaborg, and Dr. L. Winsberg for considerable assistance in the bombardment and monitoring of targets; Dr. W. F. Libby for suggesting the problem; Dr. E. W. Mueller for the use of his induction furnace; and the operating crew of the Bevatron for carrying out the bombardments.

[11] H. V. Buttlar and W. F. Libby, J. Inorg. Nuclear Chem. **1**, 75 (1955); F. Begeman, Air Force Office of Scientific Research Report AFOSR-TR-58-41, December 31, 1957 (unpublished).

[12] F. Begeman and W. F. Libby, Geochim. et Cosmochim. Acta **12**, 277 (1957); H. Craig, Phys. Rev. **105**, 1125 (1957).

PHYSICAL REVIEW VOLUME 114, NUMBER 3 MAY 1, 1959

Modified Analysis of Nucleon-Nucleon Scattering. I. Theory and *p-p* Scattering at 310 Mev*

PETER CZIFFRA,† MALCOLM H. MACGREGOR,‡ MICHAEL J. MORAVCSIK,‡ AND HENRY P. STAPP†
Radiation Laboratory, University of California, Berkeley and Livermore, California
(Received December 5, 1958)

A modified method of analyzing nucleon-nucleon scattering is discussed and applied to proton-proton scattering experiments at 310 Mev. The modified scheme is based on an explicit inclusion in all higher angular-momentum states of the terms contributed by the one-pion exchange process. This procedure is suggested by Chew's conjecture that the singularities of the scattering amplitude in the $\cos\theta$ plane (θ being the scattering angle in the center-of-mass system) that are closest to the physical region are due to the one-pion exchange process and are given by the Born approximation. Or, alternatively, in terms of ranges, the one-pion exchange contribution has the longest range of the forces contributing to the nucleon-nucleon interaction and hence should be primarily responsible for the contributions to the scattering amplitude in the high angular-momentum states. Since the only parameter in the Born approximation is the pion-nucleon coupling constant, the modified scheme can also provide a determination of this coupling constant. The application of the modified scheme to *p-p* scattering at 310 Mev indicates that the first two of the five best solutions of the conventional phase-shift analysis are more satisfactory than the others for two reasons. Firstly, their goodness-of-fit parameters improve markedly when the higher angular-momentum contributions are added, whereas those of the others remain essentially unchanged. Secondly, as a function of the coupling constant, the goodness-of-fit parameters of the first two solutions show minima close to the accepted value of the coupling constant.

1. INTRODUCTION

IT has been suggested by one of us[1] (M.J.M.) that the conventional phase shift analysis of nucleon-nucleon scattering experiments be replaced by a modified scheme in which the contribution due to the exchange of one pion is explicitly included in the scattering amplitude. This approach was motivated by some conjectures of Chew[2] on the behavior of the scattering amplitudes in the nonphysical region of the complex $\cos\theta$ plane (θ being the scattering angle in the barycentric system). Chew argues that the singularities will be restricted to the real axis and that those closest to the physical region, $-1\leq\cos\theta\leq1$, will be two symmetrically situated poles associated with contributions to the scattering amplitude of one-pion inter-

* Work done under the auspices of the U. S. Atomic Energy Commission.

† University of California Radiation Laboratory, Berkeley, California.

‡ University of California Radiation Laboratory, Livermore, California.

[1] Michael J. Moravcsik, University of California Radiation Laboratory Report UCRL-5317-T, August, 1958 (unpublished).

[2] Geoffrey F. Chew, Phys. Rev. **112**, 1380 (1958).

mediate states. If these poles are removed the remaining singularities will be, according to Chew's arguments, at least four times as far from the physical region.

Assuming these conjectures to be correct, one would expect that the contributions corresponding to more distant singularities could be adequately represented in the physical region by fewer powers of $\cos\theta$ and hence by a smaller number of partial waves. On the other hand, the contribution associated with the two near-by poles is identical with that of the lowest-order perturbation approximation to the one-pion exchange process, and is readily calculated in terms of the pion-nucleon coupling constant.

These circumstances suggest that the poles (i.e., the one-pion exchange) be explicitly included in the scattering amplitude. This should reduce the number of partial waves that are required to represent the remainder, and also permit an evaluation of the pion-nucleon coupling constant, g, which would now enter as a new parameter. This method of determining g differs somewhat from that proposed in reference 2, which uses instead the conventional phase shifts to obtain the coupling constant from nucleon-nucleon scattering experiments.

The same idea of explicitly including the one-pion exchange contribution in the higher-angular-momentum states is suggested also by the consideration that higher partial waves correspond to the forces of longer range, and the forces of longest range are due to the one-pion exchange contribution.

In the following sections some of the detailed formulas required for the application of the above scheme are presented and the results of the modified analysis of proton-proton scattering experiments at 310 Mev are discussed.

2. THE POLE CONTRIBUTION

In the conventional phase-shift analysis one expresses the scattering amplitude as a function of a limited number of phase shifts, the remaining ones being approximated by zero. This conventional expression we denote by $M(\delta)$, where M is the matrix of the scattering amplitudes corresponding to the various initial and final spin states[3,4] and δ represents the limited number of phase shifts. In the modified analysis we wish to add to $M(\delta)$ the lowest order perturbation contribution to the one-pion exchange process, that is, the pole contribution. In order to preserve the unitarity condition in the angular-momentum states represented by $M(\delta)$, the pole contributions are added only in those states that are absent in $M(\delta)$. For instance, if $M(\delta)$ contains contributions to and including $J_{\max}$ then in the modified analysis one replaces the $M(\delta)$ of the conventional analysis by

$$M(\delta,g^2)=M(\delta)+M^P(g^2,\ J>J_{\max}),\tag{2.1}$$

where $M^P(g^2,\ J>J_{\max})$ is the pole contribution from states $J>J_{\max}$. In order to compute $M(\delta,g^2)$ it is necessary to obtain the decomposition of the pole contribution into the various angular-momentum eigenstates. One method of computing this decomposition is outlined in the remainder of this section.

We define four-dimensional positive-energy Dirac spinors

$$\begin{gathered}u_r(p)=\frac{m-ip\!\!\!/}{[2m(E+m)]^{\frac{1}{2}}}\hat{u}_r,\\ \bar{u}_r(p)u_s(p)=\delta_{rs},\quad p\!\!\!/=\mathbf{p}\cdot\boldsymbol{\gamma}-p_0\gamma_0,\end{gathered}\tag{2.2}$$

where m is the nucleon mass, E the total energy of the nucleon, and

$$\hat{u}_+=\begin{bmatrix}1\\0\\0\\0\end{bmatrix},\quad \hat{u}_-=\begin{bmatrix}0\\1\\0\\0\end{bmatrix}.\tag{2.3}$$

The γ's are defined as

$$\begin{gathered}\boldsymbol{\gamma}=i\begin{pmatrix}0 & -\boldsymbol{\sigma}\\ \boldsymbol{\sigma} & 0\end{pmatrix},\quad \gamma_5=\begin{pmatrix}0 & -1\\ -1 & 0\end{pmatrix},\\ \beta=i\gamma_0=\begin{pmatrix}1 & 0\\ 0 & -1\end{pmatrix}.\end{gathered}\tag{2.4}$$

We shall also use the notation

$$x=\cos\theta,\tag{2.5}$$

where θ is the barycentric scattering angle, and

$$x_0=1+(\mu^2/mT)=1+(\mu^2/2k^2),\tag{2.6}$$

where μ is the pion mass, T the initial nucleon kinetic energy in the laboratory system, and k the barycentric nucleon momentum. For p-p scattering μ denotes the mass of the neutral pion.

In this notation the pole contribution to the M matrix can be written as

$$\begin{aligned}&M_{rs,r's'}{}^P(p,q;p',q')\\ &\quad=-\frac{g^2m^2}{2k^2E}\left[\frac{\bar{u}_r(p)\gamma_5u_{r'}(p')\bar{u}_s(q)\gamma_5u_{s'}(q')}{x_0-x}\right.\\ &\qquad\qquad\left.-\frac{\bar{u}_r(p)\gamma_5u_{s'}(q')\bar{u}_s(q)\gamma_5u_{r'}(p')}{x_0+x}\right],\end{aligned}\tag{2.7}$$

$$g^2=(2m/\mu)^2f^2\approx 14,$$

where $\mathbf{p}'$, $\mathbf{q}'$ are the initial, and $\mathbf{p}$ and $\mathbf{q}$ the final nucleon momenta. The subscripts r, r', s and s' take the values plus and minus. The matrix M^P may be written in terms of the two-dimensional Pauli matrices if we

[3] L. Wolfenstein, Phys. Rev. **96**, 1654 (1954).

[4] Stapp, Ypsilantis, and Metropolis, Phys. Rev. **105**, 302 (1957).

observe that

$$\bar{u}_r(p)\gamma_5 u_{r'}(q')=(1/2m)[\boldsymbol{\sigma}\cdot(\mathbf{p}-\mathbf{q}')]_{rr'}. \quad (2.8)$$

Using this formula and the notation

$$\mathbf{l}=(\mathbf{q}+\mathbf{q}')/\xi,\quad \mathbf{m}=(\mathbf{p}-\mathbf{p}')/\Delta,\quad \mathbf{n}=(\mathbf{q}'\times\mathbf{q})/\eta, \quad (2.9)$$

where, in the center-of-mass system,

$$\begin{aligned}\xi^2&=2k^2(1+\cos\theta),\\ \Delta^2&=2k^2(1-\cos\theta),\\ \eta^2&=k^4\sin^2\theta,\end{aligned} \quad (2.10)$$

one may express Eq. (2.7) in the form

$$\begin{aligned}M_{rs,r's'}{}^P=&-(g^2/8E)[\alpha I+(\beta+\alpha)(\boldsymbol{\sigma}^{(1)}\cdot\mathbf{l}\boldsymbol{\sigma}^{(2)}\cdot\mathbf{l}\\ &-\boldsymbol{\sigma}^{(1)}\cdot\mathbf{m}\boldsymbol{\sigma}^{(2)}\cdot\mathbf{m})-\beta(\boldsymbol{\sigma}^{(1)}\cdot\mathbf{l}\boldsymbol{\sigma}^{(2)}\cdot\mathbf{l}\\ &+\boldsymbol{\sigma}^{(1)}\cdot\mathbf{m}\boldsymbol{\sigma}^{(2)}\cdot\mathbf{m})-\alpha\boldsymbol{\sigma}^{(1)}\cdot\mathbf{n}\boldsymbol{\sigma}^{(2)}\cdot\mathbf{n}]_{rs,r's'}, \end{aligned}\quad (2.11)$$

where I is the unit matrix, $\boldsymbol{\sigma}^{(1)}$ and $\boldsymbol{\sigma}^{(2)}$ the two nucleon spin matrices, and

$$\alpha=(1+x)/(x_0+x),\quad \beta=(1-x)/(x_0-x). \quad (2.12)$$

In Eq. (2.11) the r indices refer to $\boldsymbol{\sigma}^{(1)}$ and the s indices refer to $\boldsymbol{\sigma}^{(2)}$. In the singlet-triplet representation,[5] Eq. (2.11) becomes

$$\begin{aligned}M_{11}{}^P&=M_{-1-1}{}^P=-(g^2/8E)[\alpha(1+x)-\beta(1-x)],\\ M_{10}{}^P&=M_{01}{}^P=-M_{-10}{}^P=-M_{0-1}{}^P\\ &=-(g^2\sqrt{2}/8E)(\beta+\alpha)\sin\theta,\\ M_{1-1}{}^P&=M_{-11}{}^P=-(g^2/8E)[\alpha(1-x)-\beta(1+x)],\\ M_{00}{}^P&=(g^2/4E)(\beta+\alpha)x,\\ M_{ss}{}^P&=-(g^2/4E)(\alpha+\beta).\end{aligned} \quad (2.13)$$

In order to separate the contributions from the various final angular-momentum states, one may expand these matrix elements in terms of spherical harmonics. This gives

$$M_{11}{}^P=M_{-1-1}{}^P=\frac{g^2\sqrt{\pi}}{2E}\left\{-\frac{1}{\sqrt{3}}Y_1{}^0(\theta,\phi)+(x_0-1)^2\sum_{L=1,\,L\text{ odd}}^{\infty}(2L+1)^{\frac{1}{2}}Q_L(x_0)Y_L{}^0(\theta,\phi)\right\},$$

$$M_{00}{}^P=\frac{g^2\sqrt{\pi}}{E}\left\{\frac{1}{\sqrt{3}}Y_1{}^0(\theta,\phi)-x_0(x_0-1)\sum_{L=1,\,L\text{ odd}}^{\infty}(2L+1)^{\frac{1}{2}}Q_L(x_0)Y_L{}^0(\theta,\phi)\right\},$$

$$M_{10}{}^P=-M_{0-1}{}^P=-\frac{g^2\sqrt{\pi}}{\sqrt{2}E}\left\{\left(\frac{2}{3}\right)^{\frac{1}{2}}Y_1{}^{-1}(\theta,\phi)-(x_0-1)(x_0{}^2-1)^{\frac{1}{2}}\sum_{L=1,\,L\text{ odd}}^{\infty}\left[\frac{2L+1}{L(L+1)}\right]^{\frac{1}{2}}Q_L{}^1(x_0)Y_L{}^{-1}(\theta,\phi)\right\},$$

$$M_{01}{}^P=-M_{-10}{}^P=\frac{g^2\sqrt{\pi}}{\sqrt{2}E}\left\{\left(\frac{2}{3}\right)^{\frac{1}{2}}Y_1{}^1(\theta,\phi)-(x_0-1)(x_0{}^2-1)\sum_{L=1,\,L\text{ odd}}^{\infty}\left[\frac{2L+1}{L(L+1)}\right]^{\frac{1}{2}}Q_L{}^1(x_0)Y_L{}^1(\theta,\phi)\right\}, \quad (2.14)$$

$$M_{-11}{}^P=\frac{g^2\sqrt{\pi}}{2E}(x_0{}^2-1)\sum_{L=3,\,L\text{ odd}}^{\infty}\left[\frac{2L+1}{(L+2)(L+1)L(L-1)}\right]^{\frac{1}{2}}Q_L{}^2(x_0)Y_L{}^2(\theta,\phi),$$

$$M_{1-1}{}^P=\frac{g^2\sqrt{\pi}}{2E}(x_0{}^2-1)\sum_{L=3,\,L\text{ odd}}^{\infty}\left[\frac{2L+1}{(L+2)(L+1)L(L-1)}\right]^{\frac{1}{2}}Q_L{}^2(x_0)Y_L{}^{-2}(\theta,\phi),$$

$$M_{ss}{}^P=\frac{g^2\sqrt{\pi}}{E}\left\{-Y_0{}^0(\theta,\phi)+(x_0-1)\sum_{L=0,\,L\text{ even}}^{\infty}(2L+1)^{\frac{1}{2}}Q_L(x_0)Y_L{}^0(\theta,\phi)\right\}.$$

The $Y_L{}^{L_z}(\theta,\phi)$ are the spherical harmonics as defined by Blatt and Weisskopf,[6] and the $Q_L{}^{L_z}(x_0)$ are the associated Legendre functions of the second kind as defined by Morse and Feshbach.[7]

Using Eq. (2.14) one may separate the contributions from the various final angular-momentum states. Specifically one obtains the quantities $M(L,S,L_z,S_z;S',S_z')$, defined by

$$M_{S_zS_z'}(\theta,\phi)=\textstyle\sum_L Y_L{}^{L_z}(\theta,\phi)M(L,S,L_z,S_z;S',S_z'), \quad (2.15)$$

where the primed and unprimed variables refer to initial and final states, respectively. The quantities $M(L,S,L_z,S_z;S',S_z')$ contain those contributions to M which correspond to the final orbital angular momentum L.

For the singlet case, comparison with Table III of reference 4 allows one to obtain at once the expression for the singlet amplitude α_L. For the triplet case, however, one must first separate the contributions from

[5] Henry P. Stapp, University of California Radiation Laboratory Report UCRL-3098, August, 1955 (unpublished). In Eq. (2.13) we have taken ϕ, the azimuthal scattering angle, equal to zero.

[6] J. Blatt and V. Weisskopf, *Theoretical Nuclear Physics* (J. Wiley & Sons, New York, 1952), p. 782.

[7] P. Morse and H. Feshbach, *Methods of Theoretical Physics* (McGraw-Hill Book Company, Inc., New York, 1953). Note that the recursion relations $(n+1)Q_{n+1}(x)+nQ_{n-1}(x)=(2n+1)x\times Q_n(x)$ do not hold for $n=0$. One has instead for $n=0$ the formula $Q_1(x)=xQ_0(x)-1$.

TABLE I. Goodness-of-fit parameters for p-p scattering at 310 Mev.

Set	$g^2=0$ (conventional analysis)	$g^2=9.4$	$g^2=14.4$	$g^2=19.4$	$g^2=28.8$
1	17.92	14.37	13.97	14.83	20.09
2	21.66	18.32	17.59	17.89	21.85
3	23.79	23.66	25.01	27.29	20.09
4	24.51	25.44	17.59	17.88	21.85
6	34.58	34.05	34.98	35.44	34.77

the three possible values of J that are consistent with this value of L. We express the separation of $M(L,S,L_z,S_z;S',S_z')$ into its constituent J contributions by the equation

$$M(L,S,L_z,S_z;S',S_z')=\sum_J M(J;L,S,L_z,S_z;S',S_z'). \qquad (2.16)$$

The isolation of the individual J value may be achieved by the use of the projection operators $P(J,J_z;L,S,L_z,S_z;L,S,L_z'',S_z'')$, defined by

$$\sum_{S_z''L_z''} P(J,J_z;L,S,L_z,S_z;L,S,L_z'',S_z'')\times M(L,S,L_z'',S_z'';S,S_z')=M(J;L,S,L_z,S_z,S,S_z'), \qquad (2.17)$$

where $J_z=L_z+S_z=L_z''+S_z''=S_z'+L_z'=S_z'$. The vanishing of L_z' is a consequence of the choice of coordinate system.[4] Recalling that the Clebsch-Gordan coefficients $C_{LS}(J,J_z,L_z,S_z)$ are simply the transformation matrices between different representations, one may easily see that the necessary projection operators may be expressed as

$$P(J,J_z;L,S,L_z,S_z;L,S,L_z',S_z')=C_{LS}(J,J_z;L_z,S_z)C_{LS}(J,J_z;L_z',S_z'). \qquad (2.18)$$

For the case $J=L$ the projection operator immediately isolates the contribution from α_{LL}. For the cases $J=L\pm 1$, however, the projection gives, instead, the sum of contributions from the two amplitudes α_{LJ} and α^J. However, the three values of J_z give two linearly independent equations which are readily solved. We obtain in this way the final expressions

$$\begin{aligned}
\alpha_{L,\,L+1}{}^P &= -\frac{ikg^2}{2E(2L+3)}[Q_{L+1}(x_0)-Q_L(x_0)],\\
\alpha_{L,\,L-1}{}^P &= -\frac{ikg^2}{2E(2L-1)}[Q_L(x_0)-Q_{L-1}(x_0)],\\
\alpha_{L,\,L}{}^P &= -\frac{ikg^2}{2E(2L+1)}[LQ_{L+1}(x_0)\\
&\quad +(L+1)Q_{L-1}(x_0)-(2L+1)Q_L(x_0)],\\
\alpha^{JP} &= -\frac{ikg^2}{2E(2L+1)}[J(J+1)]^{\frac{1}{2}}\\
&\quad \times[Q_{J+1}(x_0)+Q_{J-1}(x_0)-2Q_J(x_0)],\\
\alpha_L{}^P &= \frac{ikg^2}{2E}[(x_0-1)Q_L(x_0)-\delta_{L0}].
\end{aligned} \qquad (2.19)$$

The symbol δ_{L0} is the Kronecker δ function. The contribution from δ_{L0} in the S state, which arises naturally in the relativistic Born approximation, corresponds in the nonrelativistic case to the explicit δ function appearing in the potential.[8]

3. p-p SCATTERING AT 310 MEV

In this section the application of the modified procedure to p-p scattering data at 310 Mev is discussed. A conventional phase-shift analysis at this energy is given in reference 4, and this is used as a basis of comparison.

In the conventional analysis, phase shifts up through H waves were used. Our first step was to take in turn each of the five "best" solutions of that analysis and

TABLE II. Conventional ($g^2=0$) and modified ($g^2=14.4$) phase shifts[a] for p-p scattering at 310 Mev.

State	Set 1 Old	Set 1 New	Set 2 Old	Set 2 New	Set 3 Old	Set 3 New	Set 4 Old	Set 4 New	Set 6 Old	Set 6 New
$^1S_0$	−10.1	−10.9	−19.5	−22.1	−11.0	−11.2	−27.0	−22.1	−0.3	0.4
$^1D_2$	12.9	12.1	4.4	4.4	13.3	13.4	4.9	4.4	12.9	12.1
$^1G_4$	1.0	1.2	1.3	1.1	1.1	1.2	1.1	1.1	−1.1	−1.3
$^3P_0$	−14.3	−14.0	−36.1	−34.4	−4.1	−4.4	−25.4	−34.4	−64.7	−65.7
$^3P_1$	−26.7	−26.2	−11.7	−11.1	−20.0	−19.8	−7.3	−11.1	−13.4	−14.1
$^3F_3$	−4.4	−4.6	0.3	−0.5	−2.6	−3.0	1.6	−0.5	3.1	2.5
$^3H_5$	0.1	−0.4	−1.4	−1.5	0.9	0.5	−0.9	−1.5	−2.0	−2.0
$^3H_6$	1.3	1.2	1.4	1.4	−0.6	−0.3	−0.8	1.4	0.3	0.5
$^3P_2$	16.1	16.6	18.8	19.2	22.6	22.4	23.1	19.2	8.2	8.2
$^3F_2$	0.8	1.3	−0.5	0.1	−2.0	−1.8	−1.4	0.1	−2.1	−1.3
ϵ_2	−1.0	−1.4	−9.3	−8.6	1.8	1.4	−7.5	−8.6	−0.2	0.9
$^3F_4$	3.2	3.2	2.5	2.9	0.5	0.8	2.6	2.9	3.3	3.4
$^3H_4$	1.5	1.7	2.1	2.4	−1.1	−0.4	−0.7	2.4	2.2	2.3
ϵ_4	−1.2	−1.4	−1.5	−1.7	−0.9	−1.4	−0.8	−1.7	1.3	0.8

[a] Nuclear bar phase shifts in degrees as defined in reference 4.

[8] H. A. Bethe and F. de Hoffmann, *Mesons and Fields* (Row, Peterson, and Company, Evanston, 1955), Vol. II, p. 301, Eq. (13).

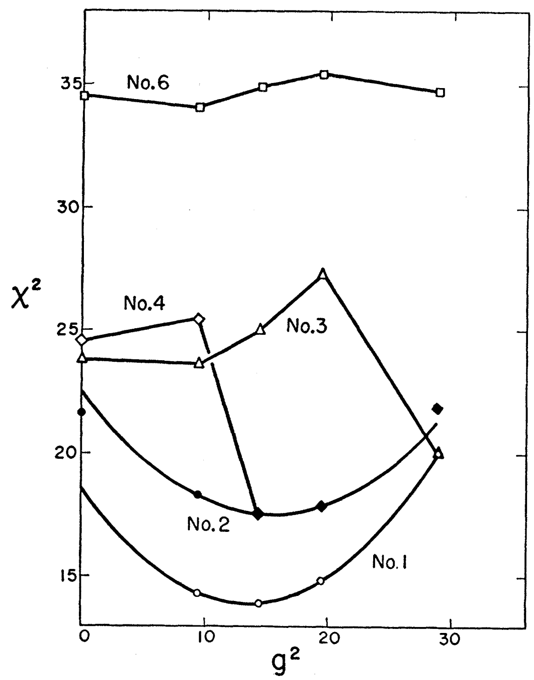

FIG. 1. Goodness-of-fit parameter *vs* pion-nucleon coupling constant for the five "best" solutions of the modified analysis of p-p scattering at 310 Mev. For Solutions 1 and 2 a parabola was drawn through the points at $g^2=9.4$, 14.4, and 19.4; these parabolas have their minima at $g^2=13.48$ and $g^2=15.42$, respectively.

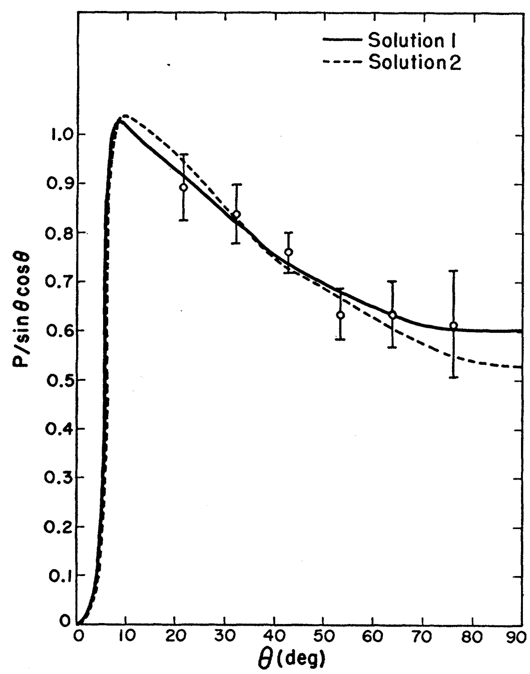

FIG. 2. Plot of $P/\sin\theta\cos\theta$ *vs* θ for Solutions 1 and 2 at $g^2=14.4$. Experimental values are shown for comparison.

simply add the pole contribution in the angular-momentum states beyond the H waves. For the coupling constant we used, in turn, the values 9.4, 14.4, 19.4, and 28.8. The goodness-of-fit parameter increased at $g^2=14.4$ by about 15 in all cases. This constituted a change of between 40% and 80%. Next, with the added pole contribution unchanged, a search was made for the new best sets of phase shifts. All partial waves up through H waves were allowed to vary. For $g^2=14.4$ we obtained what we believe to be improved sets of phase shifts.

The calculations were carried out on the IBM-704 electronic computer, the code being the same as that of reference 4 except for the inclusion of the pole contribution. The results of the new search are given in Tables I, II, and III, and in Figs. 1–7.

Table I gives the goodness-of-fit parameter χ^2 for the five new sets of solutions. In the first column are the values of χ^2 for the conventional analysis. This corresponds to the modified analysis with $g^2=0$. The various values of χ^2 are also shown in Fig. 1. For Solutions 1 and 2, parabolas through the lowest three points are also given. These have minima at $g^2=13.48$ for Solution 1 and $g^2=15.42$ for Solution 2. It will be

TABLE III. The value of the observables as determined by the phase shifts, for p-p scattering at 310 Mev, Set No. 1.

Observ-able[a]	Old value	One-pion term, old phase shifts Value	% change	One-pion term, new phase shifts Value	% change
$I_0(90°)$	3.72 mb	3.85 mb	3.5	3.72 mb	0
$r(9.1°)$	1.041	1.076	3.4	1.055	1.3
$r(11.3°)$	1.034	1.057	2.2	1.028	−0.6
$r(14.8°)$	1.079	1.090	1.0	1.058	−2.0
$r(18.6°)$	1.094	1.105	1.0	1.076	−1.7
$r(23.4°)$	1.079	1.097	1.7	1.075	−0.4
$r(31.9°)$	1.044	1.052	0.8	1.055	1.0
$r(36.0°)$	1.033	1.024	−0.9	1.042	0.9
$r(44.8°)$	1.012	0.958	−5.6	1.012	0
$r(52.4°)$	0.993	0.916	−8.4	0.988	−0.5
$r(60.8°)$	0.985	0.911	−8.1	0.980	−0.5
$r(64.0°)$	0.986	0.921	−7.1	0.983	−0.3
$r(71.4°)$	0.994	0.955	−4.1	0.992	−0.2
$r(80.2°)$	1.000	0.988	−1.2	0.999	−0.1
$s(76.2°)$	0.622	0.602	−3.3	0.603	−3.2
$s(63.9°)$	0.628	0.645	2.7	0.631	0.5
$s(53.4°)$	0.661	0.697	5.4	0.677	2.4
$s(42.9°)$	0.734	0.747	1.8	0.737	0.4
$s(32.3°)$	0.850	0.820	−3.7	0.821	−3.5
$s(21.6°)$	0.956	0.915	−4.5	0.916	−4.4
$t(23.0°)$	0.760	0.749	−1.5	0.724	−5.0
$t(25.8°)$	0.702	0.721	2.7	0.700	−0.3
$t(36.5°)$	0.519	0.570	9.8	0.576	11.0
$t(52.0°)$	0.469	0.409	−11.5	0.448	−4.7
$t(65.2°)$	0.530	0.499	−6.2	0.500	−6.0
$t(80.5°)$	0.512	0.557	8.8	0.528	3.1
$u(22.3°)$	−0.226	−0.249	−10.2	−0.213	6.1
$u(34.4°)$	−0.173	−0.152	13.8	−0.103	68.0
$u(41.8°)$	−0.006	0.007	216.7	0.050	933.3
$u(54.1°)$	0.314	0.294	−6.8	0.314	0
$u(70.9°)$	0.521	0.505	−3.2	0.517	−0.8
$u(80.1°)$	0.606	0.613	1.2	0.623	2.8
$v(25.4°)$	−1.148	−1.202	−4.7	−1.315	−14.5
$v(51.4°)$	0.011	0.095	863.6	0.005	−54.5
$v(76.3°)$	0.436	0.379	−11.5	0.381	−14.4
$\sigma_T \geqq 20°$	22.14 mb	22.14 mb	0	22.10	−0.2

[a] $r(x)=I_0(x)/I_0(90°)$; $s(x)=P(x)/\sin x\cos x$; $t(x)=1-D(x)$; $u(x)=R(x)/\cos(\frac{1}{2}x)$; $v(x)=A(x)/\sin(\frac{1}{2}x)$.

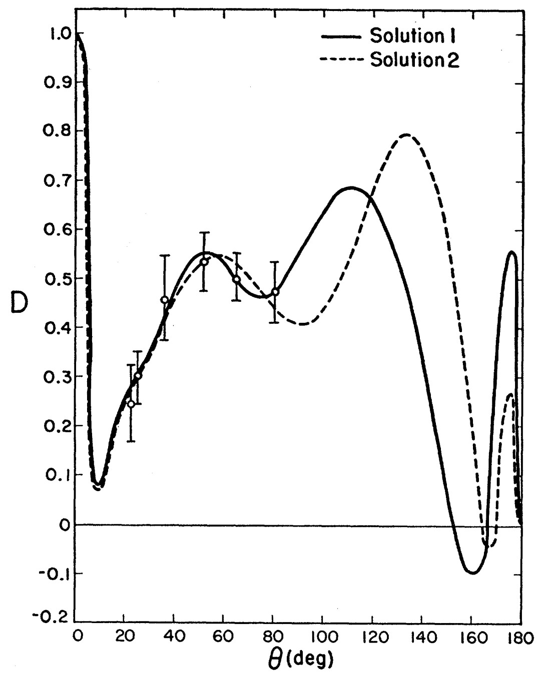

FIG. 3. Plot of D *vs* θ for Solutions 1 and 2 at $g^2=14.4$. Experimental values are shown for comparison.

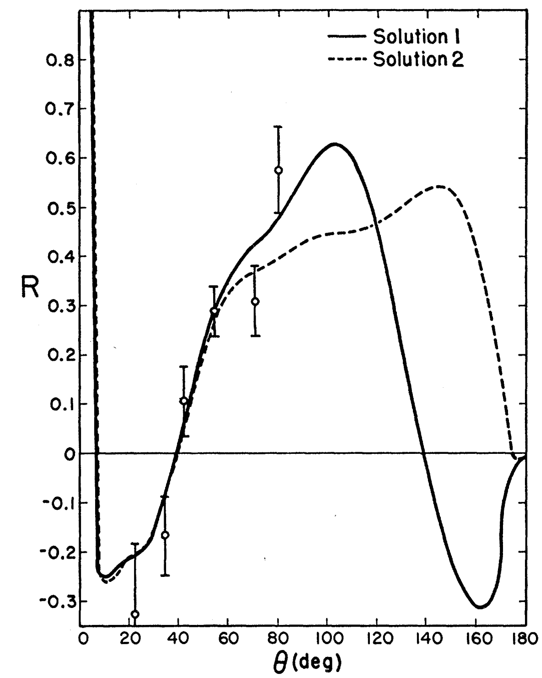

FIG. 4. Plot of R *vs* θ for Solutions 1 and 2 at $g^2=14.4$. Experimental values are shown for comparison.

observed that the plot of the goodness-of-fit parameter for Solution 4 contains only the $g^2=0$ and $g^2=9.4$ points. For the larger values of g^2 the solutions were identical with those obtained from Solution 2. This indicates that for $g^2=0$ Solution 4 was probably a relative minimum separated from Solution 2 by a rather low barrier and that the addition of the g^2 contribution either eliminated the relative minimum or distorted the contours enough to give the effect observed. Similarly Solution 3 goes over into Solution 1 at $g^2=28.8$. These effects are not surprising if one considers that even at $g^2=0$ the predictions[4] of Solutions 1 and 3 were quite similar for the various observables even in the region where no experiments exist. Similarly, the predictions of Solutions 2 and 4 at $g^2=0$ are also similar.

Table II gives the new sets of phase shifts themselves and also, for comparison, the corresponding sets from the conventional analysis. Finally, Table III gives, for set No. 1, the observables (a) as given by the conventional analysis, (b) as given by the conventional phase shifts (unchanged) plus the pole contribution in the angular-momentum states above H waves, and (c) as given by the new phase shifts plus the pole contribution in angular-momentum states above H waves. This table is given to show the detailed effect upon the observables of the modifications involved in the present scheme.

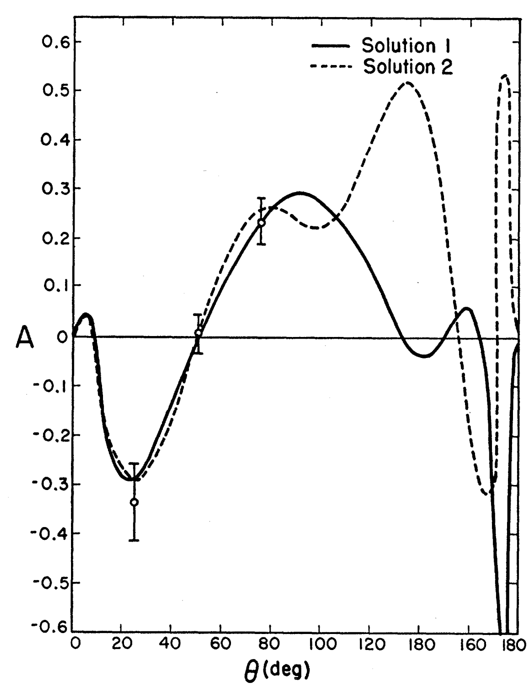

FIG. 5. Plot of A *vs* θ for Solutions 1 and 2 at $g^2=14.4$. Experimental values are shown for comparison.

Figures 2–7 give the predictions of Solutions 1 and 2 at $g^2=14.4$ for the various observables as defined in reference 5. It is clear from these figures that the two solutions differ markedly for some range in some of the observables, so that even a qualitative experiment, if properly chosen, could distinguish between the two solutions.

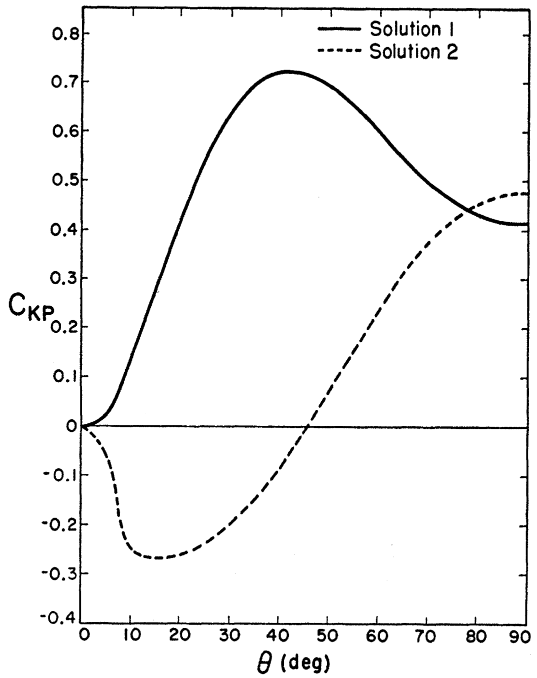

FIG. 6. Plot of C_{KP} *vs* θ for Solutions 1 and 2 at $g^2=14.4$.

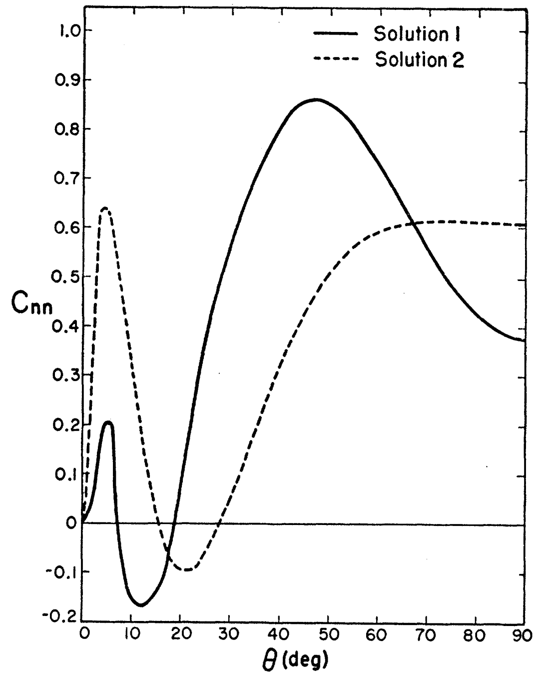

FIG. 7. Plot of C_{nn} *vs* θ for Solutions 1 and 2 at $g^2=14.4$.

4. CONCLUSIONS

The significant features of the results contained in Tables I, II, and III are as follows.

1. The goodness-of-fit parameter χ^2 decreased appreciably only for Solutions 1 and 2. This is the behavior expected of the correct set of phase shifts.

2. For solutions 1 and 2 the parameter χ^2, considered as a function of g^2, is represented by a smooth second-order function that shows a minimum near 14.4, the presently accepted value of this parameter.

3. The inclusion of the pole contribution in higher-angular-momentum states produces changes ranging from about 0% to about 80% of the experimental errors. These changes are significant enough to warrant incorporation into analyses of experiments of this nature.

4. Although the observables changed significantly, the new best sets of phase shifts differ generally by less than a degree from the solutions obtained in reference 4.

Work is under way to extend the present scheme in a number of directions. First we plan to fix the H and G phase shifts at the values given by the pole contributions, since these values do not differ markedly from the values obtained in the calculations presented here. This procedure reduces the number of free parameters and should increase the sensitivity with respect to the value of the coupling constant. Also this procedure may further help to resolve the ambiguity with regard to the various sets of phase shifts. We also plan to extend the application of the present method to other energies and to n-p scattering. Finally, work is in progress on the incorporation of the two-pion exchange contribution into the above scheme, and it is hoped that eventually other processes may also be included.

5. ACKNOWLEDGMENTS

We are indebted to Professor Geoffrey F. Chew for encouragement and helpful discussions. We are also grateful to Dr. H. Pierre Noyes and Dr. Sidney Fernbach for their active interest in our work.